

Spin-orbit coupling induced quantum droplet in ultracold Bose-Fermi mixtures

Xiaoling Cui

*Beijing National Laboratory for Condensed Matter Physics, Institute of Physics,
Chinese Academy of Sciences, Beijing, 100190, People's Republic of China*

(Dated: April 11, 2018)

Quantum droplets have intrigued much attention recently in view of their successful observations in the ultracold homonuclear atoms. In this work, we demonstrate a new mechanism for the formation of quantum droplet in heteronuclear atomic systems, i.e., by applying the synthetic spin-orbit coupling (SOC). Take the Bose-Fermi mixture for example, we show that by imposing a Rashba SOC between the spin states of fermions, the greatly suppressed Fermi pressure can enable the formation of Bose-Fermi droplets even for very weak boson-fermion attractions, which are insufficient to bound a droplet if without SOC. In such SOC-induced quantum droplets, the boson/fermion density ratio universally depends on the SOC strength, and they occur in the mean-field collapsing regime but with a negative fluctuation energy, distinct from the interaction-induced droplets found in literature. The accessibility of these Bose-Fermi droplets in ultracold Cs-Li and Rb-K mixtures is also discussed. Our results shed light on the droplet formation in a vast class of heteronuclear atomic systems through the manipulation of single-particle physics.

Self-bound droplets are ubiquitous in nature, while their quantum mechanical analogs, quantum droplets, are challenging to achieve in physical systems as their appearance requires sophisticated balance between attractive and repulsive forces. Recently, the study of quantum droplet has become a hot topic in the field of ultracold atoms. A pioneer work by Petrov showed that self-bound droplets of a two-component Bose gas can form in the mean-field collapsing regime[1], due to a balance between mean-field attraction ($\sim -n^2$, n is the density) and Lee-Huang-Yang repulsion from quantum fluctuations ($\sim n^{5/2}$), and importantly, they stay in the weak coupling regime that can effectively avoid atom loss. To date, quantum droplets have been successfully observed in Lanthanum atoms with strong dipole-dipole interaction[2–5], and in alkali boson mixtures[6–8] which exactly follow Petrov's scenario. Droplet formation has recently also been predicted in low-D[9–12] and in photonic systems[13].

Given successful explorations of quantum droplets in homonuclear systems[2–8], it naturally arises a question whether such a peculiar state exists in heteronuclear systems, especially Bose-Fermi mixtures with coexisting different statistics. Actually, in this problem the Bose-Fermi and Bose-Bose mixtures share some similarities, in that the Fermi pressure in the former naturally plays the role of boson repulsion in the latter as a repulsive force, and both systems host an additional repulsion from quantum fluctuations[1, 14]. So a Bose-Fermi droplet is expectable by fine-tuning boson-fermion attractions, as has been theoretically confirmed recently[15]. Nevertheless, one notes that the Fermi pressure scales as $\sim n^{5/3}$, which, compared to the boson repulsion ($\sim n^2$), generates higher repulsive force in the dilute limit. Accordingly, a stronger attraction in Bose-Fermi mixtures is required to form a droplet. Strong interaction can invalidate perturbative theories in treating the droplets, and inevitably induce

severe atom losses to prevent their realistic detection in experiments.

In this work, we demonstrate a new route to stabilize the quantum droplet, i.e., by introducing the spin-orbit coupling (SOC). In the past few years, cold atoms experiments have successfully realized the synthetic 1D[16–26] and 2D[27–29] types of SOC, and the highly symmetric SOC including the Rashba and isotropic types have also been theoretically proposed[30–37]. Our work is simply motivated by the fact that SOC can significantly modify the single-particle physics in low-energy space. In particular, for a highly symmetric SOC, the resulted single-particle ground state degeneracy in combination with interactions has been found to induce intriguing dimer[38–43], trimer[44–46] and many-body physics[47]. Here, we point out another dramatic effect of the highly symmetric SOC, namely, in driving the formation of stable Bose-Fermi droplets in weak coupling regime. The associated mechanism can be generalized to various other heteronuclear systems in different dimensions.

To be concrete, we consider a Rashba spin-orbit coupled Fermi gas spin-selectively interacting with a Bose gas, which is described by the following Hamiltonian

$$\begin{aligned}
 H = & \sum_{\mathbf{k}} \epsilon_{\mathbf{k}}^b b_{\mathbf{k}}^\dagger b_{\mathbf{k}} + \frac{U_{bb}}{V} \sum_{\mathbf{k}, \mathbf{k}', \mathbf{Q}} b_{\mathbf{k}}^\dagger b_{\mathbf{Q}-\mathbf{k}}^\dagger b_{\mathbf{Q}-\mathbf{k}'} b_{\mathbf{k}'} \\
 & + \sum_{\mathbf{k}, \alpha} \epsilon_{\mathbf{k}}^f f_{\mathbf{k}, \alpha}^\dagger f_{\mathbf{k}, \alpha} + \frac{\lambda}{m_f} \sum_{\mathbf{k}} \left((k_x - ik_y) f_{\mathbf{k}, \uparrow}^\dagger f_{\mathbf{k}, \downarrow} + h.c. \right) \\
 & + \frac{U_{bf}}{V} \sum_{\mathbf{k}, \mathbf{k}', \mathbf{Q}} f_{\mathbf{k}, \uparrow}^\dagger b_{\mathbf{Q}-\mathbf{k}}^\dagger b_{\mathbf{Q}-\mathbf{k}'} f_{\mathbf{k}', \uparrow}. \quad (1)
 \end{aligned}$$

Here $b_{\mathbf{k}}^\dagger$ and $f_{\mathbf{k}, \alpha}^\dagger$ create a boson and a spin- α ($=\uparrow, \downarrow$) fermion, respectively, with energy $\epsilon_{\mathbf{k}}^b = \mathbf{k}^2/2m_b$ and $\epsilon_{\mathbf{k}}^f = \mathbf{k}^2/2m_f$; U_{bb} and U_{bf} are respectively the bare boson-boson and boson-fermion interactions, which can be related to scattering lengths a_{bb} and a_{bf} via renormalization equations, for instance, $1/U_{bf} = 1/g_{bf} -$

$(1/V) \sum_{\mathbf{k}} 1/(2m_b f \mathbf{k}^2)$, with $g_{bf} = 2\pi a_{bf}/m_{bf}$, $m_{bf} = m_b m_f / (m_b + m_f)$, and V the volume. Here we consider a Rashba SOC between two-species fermions with strength λ , and the resulted single-particle eigenstate is created by $f_{\mathbf{k},\sigma}^\dagger = \sum_{\alpha} \gamma_{\mathbf{k},\sigma}^{\alpha} f_{\mathbf{k},\alpha}^\dagger$, where $\sigma = \pm$ is the index of helicity branch, $\gamma_{\mathbf{k},\pm}^\uparrow = \pm e^{\pm i\phi_{\mathbf{k}}/2}/\sqrt{2}$, $\gamma_{\mathbf{k},\pm}^\downarrow = e^{\pm i\phi_{\mathbf{k}}/2}/\sqrt{2}$, $\phi_{\mathbf{k}} = \arg(k_x, k_y)$; the corresponding eigen-energy is $\epsilon_{\mathbf{k},\sigma}^f = ((k_{\perp} + \sigma\lambda)^2 + k_z^2)/(2m_f)$ (here $k_{\perp} = \sqrt{k_x^2 + k_y^2}$), which gives a $U(1)$ ground state degeneracy in \mathbf{k} -space with $k_{\perp} = \lambda$. For brevity, we take $\hbar = 1$ throughout the paper.

In this work, we consider weakly interacting bosons with small $a_{bb}(> 0)$, and a weak attraction between boson and spin- \uparrow fermion with small $a_{bf}(< 0)$. Given the boson and fermion densities n_b and n_f , the energy density of the system can be written as

$$\mathcal{E}(n_b, n_f) = \mathcal{E}_b + \mathcal{E}_f + \mathcal{E}_{bf}, \quad (2)$$

here $\mathcal{E}_b = (2\pi a_{bb}/m_b)n_b^2[1 + (128/15\pi^{1/2})(n_b a_{bb}^3)^{1/2}]$ is the ground state energy of the Bose gas with Lee-Huang-Yang correction. \mathcal{E}_f is the Fermi sea energy under Rashba SOC:

$$\mathcal{E}_f = \frac{1}{V} \sum_{\mathbf{k},\sigma} \epsilon_{\mathbf{k},\sigma}^f \theta(E_f - \epsilon_{\mathbf{k},\sigma}^f), \quad (3)$$

with $E_f \equiv \lambda_f^2/(2m_f)$ the Fermi energy and λ_f the Fermi momentum, determined by the density constraint $n_f = \frac{1}{V} \sum_{\mathbf{k},\sigma} \theta(E_f - \epsilon_{\mathbf{k},\sigma}^f)$. $\mathcal{E}_{bf} = \mathcal{E}_{bf}^{(1)} + \mathcal{E}_{bf}^{(2)}$ is the interaction energy between bosons and fermions, here $\mathcal{E}_{bf}^{(1)} = g_{bf} n_b n_{f,\uparrow}$ is the mean-field interaction energy, and $\mathcal{E}_{bf}^{(2)}$ ($\sim g_{bf}^2$) is the lowest-order correction due to density fluctuations, which can be obtained from the second-order perturbation theory as:

$$\mathcal{E}_{bf}^{(2)} = n_b \frac{g_{bf}^2}{V} \sum_{\mathbf{k}} \left(n_{f,\uparrow} \frac{2m_{bf}}{\mathbf{k}^2} - \frac{\epsilon_{\mathbf{k}}^b}{\omega_{\mathbf{k}}} \sum_{\mathbf{q},\sigma,\sigma'} \frac{1}{4V} \frac{\theta(E_f - \epsilon_{\mathbf{q},\sigma}^f) \theta(\epsilon_{\mathbf{k}+\mathbf{q},\sigma'}^f - E_f)}{\omega_{\mathbf{k}} + \epsilon_{\mathbf{k}+\mathbf{q},\sigma'}^f - \epsilon_{\mathbf{q},\sigma}^f} \right) \quad (4)$$

Here $\omega_{\mathbf{k}} = \sqrt{\epsilon_{\mathbf{k}}^b(\epsilon_{\mathbf{k}}^b + 8\pi n_b a_{bb}/m_b)}$ is the Bogoliubov excitation energy of bosons. In the limit of $\lambda \rightarrow 0$, our result recovers the perturbative energy of Bose-Fermi mixtures without SOC[14].

Given $\mathcal{E}(n_b, n_f)$ in (2), one can obtain the chemical potentials $\mu_b = \partial\mathcal{E}/\partial n_b$, $\mu_f = \partial\mathcal{E}/\partial n_f$, and the pressure density $\mathcal{P} = \mathcal{P}_b + \mathcal{P}_f + \mathcal{P}_{bf}$, where

$$\mathcal{P}_b = n_b \frac{\partial\mathcal{E}_b}{\partial n_b} - \mathcal{E}_b; \quad \mathcal{P}_f = n_f \frac{\partial\mathcal{E}_f}{\partial n_f} - \mathcal{E}_f; \quad (5)$$

$$\mathcal{P}_{bf} = \mathcal{P}_{bf}^{(1)} + \mathcal{P}_{bf}^{(2)};$$

$$\mathcal{P}_{bf}^{(i)} = n_b \frac{\partial\mathcal{E}_{bf}^{(i)}}{\partial n_b} + n_f \frac{\partial\mathcal{E}_{bf}^{(i)}}{\partial n_f} - \mathcal{E}_{bf}^{(i)} \quad (i = 1, 2); \quad (6)$$

Here \mathcal{P}_b (\mathcal{P}_f) is the pressure caused by individual bosons (fermions), \mathcal{P}_{bf} is due to boson-fermion interactions and contributed from both the mean-field ($\mathcal{P}_{bf}^{(1)}$) and the quantum fluctuation ($\mathcal{P}_{bf}^{(2)}$) parts. The introduction of SOC will not change \mathcal{P}_b and $\mathcal{P}_{bf}^{(1)}$, but will strongly modify \mathcal{P}_f and $\mathcal{P}_{bf}^{(2)}$ as shown below.

Before proceeding, we should note that a stable ground state droplet occurs when the following conditions are simultaneously satisfied:

- (i) $\mathcal{E} < 0$, $\mathcal{P} = 0$;
- (ii) $\mu_b \frac{\partial\mathcal{P}}{\partial n_b} = \mu_f \frac{\partial\mathcal{P}}{\partial n_f}$;
- (iii) $\frac{\partial\mu_b}{\partial n_b} > 0$, $\frac{\partial\mu_f}{\partial n_f} > 0$, $\frac{\partial\mu_b}{\partial n_b} \frac{\partial\mu_f}{\partial n_f} > \left(\frac{\partial\mu_b}{\partial n_b}\right)^2$

here the condition (i) describes a self-bound object that is in equilibrium with vacuum, a characteristic feature of droplet[1]; condition (ii) further searches for the ground state droplet with minimal energy[15]; and (iii) ensures the droplet be stable against density fluctuations.

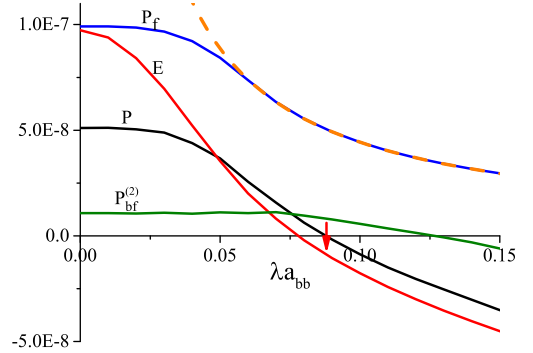


FIG. 1. \mathcal{E} , \mathcal{P} , \mathcal{P}_f and $\mathcal{P}_{bf}^{(2)}$ [in units of $m_b a_{bb}^5 / (2\pi V)$] as functions of λa_{bb} . Here we take $n_b a_{bb}^3 = 2 \times 10^{-5}$, $n_f a_{bb}^3 = 10^{-4}$, $a_{bf} = -3a_{bb}$, and $m_b/m_f = 133/6$. The red arrow marks the location where the droplet condition (i) is satisfied. The orange dashed line shows fit to \mathcal{P}_f according to Eq.7.

To gain the first insight on how a Rashba SOC affect the droplet formation, in Fig.1 we take $^{133}\text{Cs}-^6\text{Li}$ system and show its energy \mathcal{E} , pressure \mathcal{P} and pressure components \mathcal{P}_f , $\mathcal{P}_{bf}^{(2)}$ as functions of SOC strength λ , for a given attraction $a_{bf} = -3a_{bb}$ and given densities $n_b a_{bb}^3 = 2 \times 10^{-5}$, $n_f a_{bb}^3 = 10^{-4}$. It can be seen that as increasing λ from zero, both \mathcal{E} and \mathcal{P} decrease monotonically, such that at a critical $\lambda_c a_{bb} \sim 0.75$, \mathcal{P} can reduce to zero with a negative \mathcal{E} , as marked by red arrow in Fig.1, which gives a droplet solution satisfying condition (i). During this process, \mathcal{P}_f and $\mathcal{P}_{bf}^{(2)}$ also decrease, while the reduction of total \mathcal{P} mainly comes from \mathcal{P}_f , since $\mathcal{P}_{bf}^{(2)}$ varies in a relatively smaller scale.

The suppressed Fermi pressure (\mathcal{P}_f) by Rashba SOC can be attributed to the $U(1)$ ground state degeneracy

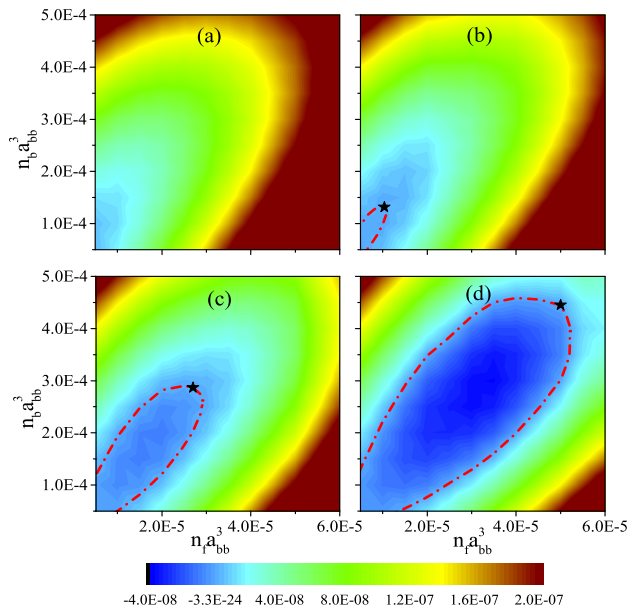


FIG. 2. Contour plots of \mathcal{P} [in unit of $m_b a_{bb}^5 / (2\pi V)$] in the $(n_f a_{bb}^3, n_b a_{bb}^3)$ plane for different SOC strengths: $\lambda a_{bb} = 0.02(a)$, $0.06(b)$, $0.08(c)$, $0.1(d)$. The red dashed-dot lines in (b,c,d) denote zero-pressure loops, and the black stars mark the locations of ground state droplets satisfying condition (ii). Here we take $a_{bf} = -3a_{bb}$ and $m_b/m_f = 133/6$.

and thus the enhanced density-of-state $\rho(E)$ at low E , which approaches a constant ($\sim m_f \lambda$) as in an effective 2D geometry, rather than zero as in the usual 3D case. As a result, in the presence of SOC, more fermions can be accommodated in the low- E space and for a given n_f this greatly suppresses the total energy and the Fermi pressure. Specifically, in the low-density or strong-SOC regime where only the lower helicity branch is occupied, i.e., $n_f < n_{f,c} \equiv \lambda^3/4\pi$, we have $\lambda_f = \sqrt{4\pi n_f/\lambda}$ and

$$\mathcal{E}_f = \mathcal{P}_f = \frac{\pi}{\lambda m_f} n_f^2. \quad (7)$$

This shows that the presence of Rashba SOC can fundamentally alter the energy(pressure)-density scaling relation, from $\sim n_f^{5/3}$ in the usual case, to $\sim n_f^2$. This greatly suppresses \mathcal{E} and \mathcal{P} for a dilute Fermi gas (with small n_f). Moreover, Eq.7 shows that \mathcal{E} , \mathcal{P} can be further reduced by increasing SOC strength λ , as also shown in Fig.1.

Given the robust single-particle physics modified by Rashba SOC, the suppression of \mathcal{P} should generally apply to all boson/fermion densities. In Fig.2, we show the contour plots of $\mathcal{P}(n_b, n_f)$ for Cs-Li system taking a fixed $a_{bf} = -3a_{bb}$ and several different values of λa_{bb} . At $\lambda a_{bb} = 0.02$ (Fig.2(a)), \mathcal{P} is always positive, while it can be effectively reduced when increasing λa_{bb} to 0.06(Fig.2(b)), where it touches zero along a small loop in (n_b, n_f) plane and becomes negative inside. Further increasing λa_{bb} to 0.08 and 0.1 (Fig.2(c,d)), \mathcal{P} is fur-

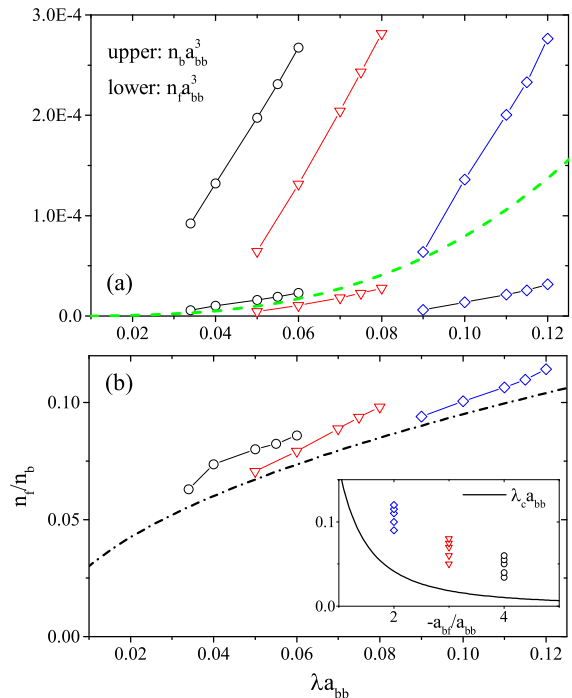


FIG. 3. Boson and fermion densities (a) and their ratios (b) as functions of λa_{bb} for the ground state droplets at different scattering lengths $a_{bf}/a_{bb} = -4$ (black circles), -3 (red triangles) and -2 (blue diamonds). The green dashed line in (a) shows the critical fermion density $n_{f,c} = \lambda^3/(4\pi)$, below which only the lower helicity branch is occupied. In (b), the orange dashed-dot line shows fit to Eq.9; in the inset, the line shows critical λ_c for mean-field collapse (see Eq.8), and the points shows actual λ for the data shown in the main plot. Here $m_b/m_f = 133/6$.

ther reduced and the zero-pressure loop becomes even enlarged. On each loop in (b-d), the location of ground state droplet following condition (ii) is further marked by a black star, and we have checked that all these solutions are with $\mathcal{E} < 0$. In addition, because the stars all locate at the top right corner of the loops, we have $\partial\mathcal{P}/\partial n_b > 0$ and $\partial\mathcal{P}/\partial n_f > 0$, which automatically ensure the satisfaction of condition (iii). Therefore they represent stable ground-state droplets satisfying all conditions (i-iii).

Repeating the same procedure for different attraction strengths $a_{bf}/a_{bb} = -2, -3, -4$, we show in Fig.3 the boson/fermion densities and their ratios as functions of λ for the ground state Cs-Li droplets. As shown in Fig.3(a), for $a_{bf} = -4a_{bb}$ (black circles), the droplets start to form at small $\lambda a_{bb} \sim 0.03$ with fermions occupying both the lower and upper helicity branches (i.e., $n_f > n_{f,c} \equiv \lambda^3/4\pi$), thus these droplets are mainly interaction-induced similar to those without SOC[15]. Gradually reducing attraction to $a_{bf} = -3a_{bb}$ (red triangles), the droplets move to larger λ and n_f starts to drop below $n_{f,c}$. For small attraction $a_{bf} = -2a_{bb}$ (blue

diamonds), the droplet appears at $\lambda a_{bb} \geq 0.09$ with $n_f \ll n_{f,c}$, i.e., the fermions are located near the bottom of lower helicity branch with U(1) ground state degeneracy. Such droplet formation crucially relies on the suppressed Fermi pressure by Rashba SOC (see Eq.7), and can only appear for strong SOC and weak attractions. Thus we term it as the SOC-induced droplet, in order to distinguish from the interaction-induced ones at small or zero SOC. Below we will extract several unique features for such kind of droplet.

First, given the fermion energy in Eq.7, we see that SOC can conveniently tune the mean-field stability, and a mean-field collapse occurs for sufficiently large λ at

$$\lambda > \lambda_c = \frac{8m_b m_f}{(m_b + m_f)^2} \frac{a_{bb}}{a_{bf}^2}. \quad (8)$$

The dependence of λ_c on a_{bf} is plotted in the inset of Fig.3(b), and this qualitatively explains why a stronger SOC is required for droplet formation at weaker attractions, as shown in Fig.3(a). Secondly, by requiring a minimal mean-field energy like in Bose-Bose mixtures[1], we obtain an optimal boson/fermion density ratio as

$$\left(\frac{n_f}{n_b}\right)_{\text{op}} = \sqrt{\frac{2m_f}{m_b}} \sqrt{\lambda a_{bb}}. \quad (9)$$

This shows a universal dependence of boson/fermion density ratio on the SOC strength, which is one of characteristic features of the SOC-induced droplet. We see from Fig.3(b) that Eq.9 can well predict the actual density ratio for the SOC-induced droplets at $a_{bf} = -2a_{bb}$ (with small discrepancy attributed to quantum fluctuation effect), but deviate largely from that of the interaction-induced ones at stronger attraction $a_{bf} = -4a_{bb}$.

The SOC-induced droplets also significantly differ from the interaction-induced ones in quantum fluctuations. To compare the fluctuation effects for all sets of parameters, we investigate the relative ratio $R \equiv \mathcal{E}_{bf}^{(2)}/|\mathcal{E}_{bf}^{(1)}|$, which quantity can also be used to judge the validity of second-order perturbation theory. In Fig.4, we plot the energy \mathcal{E} and associated ratio R for the droplet solutions in Fig.3. One can see that at given a_{bf} , \mathcal{E} monotonically decrease as increasing λ . For the same window of $|\mathcal{E}| \in [2 \times 10^{-9}, 3 \times 10^{-8}]$, R can range within [12%, 20%] for $a_{bf} = -4a_{bb}$, while can be reduced to [3%, 10%] for a weaker attraction $a_{bf} = -3a_{bb}$. For the SOC-induced droplet at $a_{bf} = -2a_{bb}$, R turns negative and its absolute value can be even smaller ($\in [0, 5\%]$).

Three remarks are in order. First, the fact that the SOC-induced droplets host sufficiently small $|R|$ is associated with their appearance in the weak coupling regime, i.e., small a_{bf} , which guarantees the validity of perturbative treatment in this problem as well as the practical stability in experiments. In comparison, the interaction-induced Bose-Fermi droplets have much higher R [48].

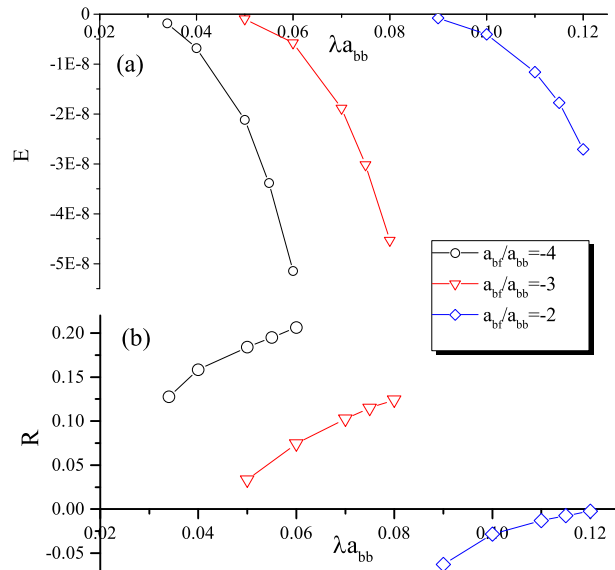


FIG. 4. Energy density \mathcal{E} [in unit of $m_b a_{bb}^5 / (2\pi V)$] (a) and the ratio $R \equiv \mathcal{E}_{bf}^{(2)}/|\mathcal{E}_{bf}^{(1)}|$ (b) as functions of λ for the droplet solutions in Fig.3.

Secondly, the SOC-induced droplets can exhibit a negative fluctuation energy $\mathcal{E}_{bf}^{(2)} < 0$, which is very rare in 3D systems. This is, again, attributed to the enhanced DoS by Rashba SOC, such that more fermions can be excited near the ground-state manifold with small excitation energy and the second term in Eq. 4 can dominate to produce a negative $\mathcal{E}_{bf}^{(2)}$. Similar effect produced by Rashba SOC have been shown to enhance the quantum depletion of a 3D Bose condensate[49, 50]. Finally, despite of a negative $\mathcal{E}_{bf}^{(2)}$, the fluctuation pressure $\mathcal{P}_{bf}^{(2)}$ still keeps positive given $\partial \mathcal{E}_{bf}^{(2)} / \partial n_f > 0$. This is why such droplet can be stabilized in the mean-field collapsing regime with $\lambda > \lambda_c$, see the inset of Fig.3(b).

Now we discuss the accessibility of SOC-induced Bose-Fermi droplets in ultracold ^{133}Cs - ^6Li and ^{87}Rb - ^{40}K mixtures. For a laser-generated SOC, typically the maximum λ is given by the wave vector of two counter-propagating lasers, i.e., $\lambda_{\text{max}} \sim 2\pi/1000 \text{ nm}^{-1}$. For Cs-Li mixtures near 892G Feshbach resonance[51], Cs-Cs scattering length $a_{bb} \sim 15\text{nm}$, giving $\lambda_{\text{max}} a_{bb} \sim 0.1$. According to Fig.3, a Cs-Li droplet can form at $a_{bf} = -2a_{bb} = -30\text{nm}$, with densities $n_f = 0.1n_b = 4 \times 10^{12} \text{ cm}^{-3}$. For Rb-K mixtures near 546G resonance[52], given a smaller Rb-Rb scattering length $a_{bb} \sim 5\text{nm}$, we have $\lambda_{\text{max}} a_{bb} \sim 0.033$. According to Eqs.(8,9), the minimum attraction required for mean-field collapse is $a_{bf} \sim -7.6a_{bb} \sim 40\text{nm}$, and the optimal density ratio in the droplet is $n_f/n_b \sim 0.17$. We note that n_b is much larger than n_f in both Cs-Li and Rb-K droplets, similar to Bose polaron systems as have been realized in cold atoms without SOC[52-54].

In summary, we have demonstrated the formation of Bose-Fermi droplets in the weak coupling regime driven by a Rashba SOC between the spin states of fermions. The SOC-induced droplets feature a negative fluctuation energy, while occur in the mean-field collapsing regime with a positive fluctuation pressure, distinct from the interaction-induced ones studied in literature. Moreover, the boson/fermion density ratio universally depends on the strength of Rashba SOC, which property can be detected in experiments. Such SOC-induced droplet has a number of implications as below. First, it offers an ideal platform to study the topological edge states when further combine SOC with interactions, since the droplet configuration naturally provides surface/boundary for cold atoms without resorting to external potentials. Moreover, this work reveals the importance of single-particle physics in engineering quantum droplets, and the associated mechanism can be generalized to a vast class of heteronuclear atomic systems in various geometries. In particular, this work sheds light on the droplet formation even in Fermi-Fermi mixtures and in mixed dimensions.

We thank D. Petrov for stimulating discussions on droplets. This work is supported by the National Key Research and Development Program of China (2016YFA0300603), and the National Natural Science Foundation of China (No.11622436, No.11421092, No.11534014).

-
- [1] D.S. Petrov, Phys. Rev. Lett. **115**, 155302 (2015).
- [2] I. Ferrier-Barbut, H. Kadau, M. Schmitt, M. Wenzel, and T. Pfau, Phys. Rev. Lett. **116**, 215301 (2016).
- [3] M. Schmitt, M. Wenzel, B. Bttcher, I. Ferrier-Barbut, and T. Pfau, Nature **539**, 259 (2016).
- [4] I. Ferrier-Barbut, M. Schmitt, M. Wenzel, H. Kadau, and T. Pfau, J. Phys. B **49**, 214004 (2016).
- [5] L. Chomaz, S. Baier, D. Petter, M.J. Mark, F. Wächtler, L. Santos, and F. Ferlaino, Phys. Rev. X **6**, 041039 (2016).
- [6] C.R. Cabrera, L. Tanzi, J. Sanz, B. Naylor, P. Thomas, P. Cheiney, and L. Tarruell, Science **359**, 301 (2018).
- [7] P. Cheiney, C. R. Cabrera, J. Sanz, B. Naylor, L. Tanzi, L. Tarruell, arXiv:1710.11079.
- [8] G. Semeghini, G. Ferioli, L. Masi, C. Mazzinghi, L. Wolswijk, F. Minardi, M. Modugno, G. Modugno, M. Inguscio, M. Fattori, arXiv:1710.10890.
- [9] D.S. Petrov and G. Astrakharchik, Ultradilute low-dimensional liquids, Phys. Rev. Lett. **117**, 100401 (2016).
- [10] C. Mishra, D. Edler, F. Wächtler, R. Nath, S. Sinha, and L. Santos, Phys. Rev. Lett. **119**, 050403 (2017).
- [11] Y. Sekino, Y. Nishida, Phys. Rev. A **97**, 011602(R) (2018).
- [12] A. Pricoupenko and D. S. Petrov, arxiv: 1802.02113.
- [13] N. Westerberg, K. E. Wilson, C. W. Duncan, D. Faccio, E. M. Wright, P. Öhberg, M. Valiente, arxiv:1801.08539.
- [14] L. Viverit and S. Giorgini, Phys. Rev. A **66**, 063604 (2002).
- [15] T. Karpiuk, D. Rakshit, M. Brewczyk, and M. Gajda, arxiv: 1801.00346.
- [16] Y.-J. Lin, K. Jiménez-García and I. B. Spielman, Nature (London) **471**, 83 (2011).
- [17] Y.-J. Lin, R. L. Compton, K. Jiménez-García, W. D. Phillips, J. V. Porto and I. B. Spielman, Nat. Phys. **7**, 531 (2011).
- [18] J.-Y. Zhang, S.-C. Ji, Z. Chen, L. Zhang, Z.-D. Du, B. Yan, G.-S. Pan, B. Zhao, Y.-J. Deng, H. Zhai, S. Chen and J.-W. Pan, Phys. Rev. Lett. **109**, 115301 (2012).
- [19] R. A. Williams, L. J. LeBlanc, K. Jiménez-García, M. C. Beeler, A. R. Perry, W. D. Phillips and I. B. Spielman, Science **335**, 314 (2012).
- [20] P. Wang, Z.-Q. Yu, Z. Fu, J. Miao, L. Huang, S. Chai, H. Zhai and J. Zhang, Phys. Rev. Lett. **109**, 095301 (2012).
- [21] L. W. Cheuk, A. T. Sommer, Z. Hadzibabic, T. Yefsah, W. S. Bakr and M. W. Zwierlein, Phys. Rev. Lett. **109**, 095302 (2012).
- [22] C. Qu, C. Hamner, M. Gong, C. Zhang and P. Engels, Phys. Rev. A **88**, 021604(R) (2013).
- [23] M. C. Beeler, R. A. Williams, K. Jiménez-García, L. J. LeBlanc, A. R. Perry and I. B. Spielman, Nature (London) **498**, 201 (2013).
- [24] J. -Y Zhang, S.-C. Ji, L. Zhang, Z.-D. Du, W. Zheng, Y.-J. Deng, H. Zhai, S. Chen, and J.-W. Pan, Nat. Phys. **10**, 314 (2014).
- [25] R. A. Williams, M. C. Beeler, L. J. LeBlanc, K. Jimenez-Garcia, and I. B. Spielman, Phys. Rev. Lett. **111**, 095301 (2013)
- [26] Z. Fu, L. Huang, Z. Meng, P. Wang, L. Zhang, S. Zhang, H. Zhai, P. Zhang, and J. Zhang, Nat. Phys. **10**, 110 (2014).
- [27] L. Huang, Z. Meng, P. Wang, P. Peng, S.-L. Zhang, L. Chen, D. Li, Q. Zhou, J. Zhang, Nat. Phys. **12**, 540 (2016).
- [28] Z. Meng, L. Huang, P. Peng, D. Li, L. Chen, Y. Xu, C. Zhang, P. Wang, J. Zhang, Phys. Rev. Lett. **117**, 235304 (2016).
- [29] Z. Wu, L. Zhang, W. Sun, X.-T. Xu, B.-Z. Wang, S.-C. Ji, Y. Deng, S. Chen, X.-J. Liu, J.-W. Pan, Science **354**, 83 (2016).
- [30] D. L. Campbell, G. Juzeliūnas, and I. B. Spielman, Phys. Rev. A **84**, 025602 (2011).
- [31] J. D. Sau, R. Sensarma, S. Powell, I. B. Spielman, and S. Das Sarma, Phys. Rev. B **83**, 140510(R) (2011).
- [32] Z. F. Xu and L. You, Phys. Rev. A **85**, 043605 (2012).
- [33] X.-J. Liu, K. T. Law, and T. K. Ng, Phys. Rev. Lett. **112**, 086401 (2014).
- [34] B. M. Anderson, I. B. Spielman, and G. Juzeliūnas, Phys. Rev. Lett. **111**, 125301 (2013).
- [35] Z.-F. Xu, L. You, and M. Ueda, Phys. Rev. A **87**, 063634 (2013)
- [36] B. M. Anderson, G. Juzeliūnas, V. M. Galitski and I. B. Spielman, Phys. Rev. Lett. **108**, 235301 (2012).
- [37] B. M. Anderson, I. B. Spielman and G. Juzeliūnas, , Phys. Rev. Lett. **111**, 125301 (2013).
- [38] J. P. Vyasankere and V. B. Shenoy, Phys. Rev. B **83**, 094515 (2011).
- [39] X. Cui, Phys. Rev. A **85**, 022705 (2012).
- [40] P. Zhang, L. Zhang, W. Zhang, Phys. Rev. A **86**, 042707 (2012).
- [41] Y. Wu and Z. Yu, Phys. Rev. A **87**, 032703 (2013).
- [42] S.-J. Wang and C. H. Greene, Phys. Rev. A **91**, 022706

- (2015).
- [43] Q. Guan, D. Blume, Phys. Rev. A **94**, 022706 (2016).
- [44] Z. Y. Shi, X. Cui, H. Zhai, Phys. Rev. Lett. **112**, 013201 (2014).
- [45] Z. Y. Shi, H. Zhai, X. Cui, Phys. Rev. A **91**, 023618 (2015).
- [46] X. Cui and W. Yi, Phys. Rev. X **4**, 031026 (2014).
- [47] See reviews: H. Zhai, Int. J. Mod. Phys. B **26**, 1230001 (2012); *ibid*, Rep. Prog. Phys. **78**, 026001 (2015); V. Galitski, I. B. Spielman, Nature (London) **494**, 49 (2013); N. Goldman, G. Juzeliūnas, P. Öhberg, I. B. Spielman, Rep. Prog. Phys. **77**, 126401 (2014); X. Zhou, Y. Li, Z. Cai, C. Wu, J. Phys. B: At. Mol. Opt. Phys. **46**, 134001 (2013); W. Yi, W. Zhang, X. Cui, Science China Physics, Mechanics and Astronomy **58**, 1 (2015).
- [48] We note that the minimal R can be as large as 27% for Cs-Li droplets without SOC[15].
- [49] T. Ozawa and G. Baym, Phys. Rev. Lett. **109**, 025301 (2012).
- [50] X. Cui and Q. Zhou, Phys. Rev. A **87**, 031604 (R) (2013).
- [51] B.J. DeSalvo, K. Patel, J. Johansen, C. Chin, Phys. Rev. Lett. **119**, 233401 (2017).
- [52] M.-G. Hu, M. J. Van de Graaff, D. Kedar, J. P. Corson, E. A. Cornell, D. S. Jin, Phys. Rev. Lett. **117**, 055301 (2016).
- [53] N. B. Jørgensen, L. Wacker, K. T. Skalmstang, M. M. Parish, J. Levinsen, R. S. Christensen, G. M. Bruun, J. J. Arlt, Phys. Rev. Lett. **117**, 055302 (2016).
- [54] F. Schmidt, D. Mayer, Q. Bouton, D. Adam, T. Lausch, N. Spethmann, A. Widera, arXiv:1802.08702.